A Titanium–Organic Framework as an Exemplar of Combining the Chemistry of Metal– and Covalent–Organic Frameworks

Ha L. Nguyen,[†,‡] Felipe Gándara,[§] Hiroyasu Furukawa,[†,∥] Tan L. H. Doan,[⊥] Kyle E. Cordova,[†,∥] and Omar M. Yaghi*,[†,∥]

[†]Department of Chemistry, University of California-Berkeley; Materials Sciences Division, Lawrence Berkeley National Laboratory; Kavli Energy NanoSciences Institute at Berkeley; and Berkeley Global Science Institute, Berkeley, California 94720, United States
[‡]Vietnam National University-Ho Chi Minh City (VNU-HCM), Ho Chi Minh City 721337, Vietnam
[§]Department of New Architectures in Materials Chemistry, Materials Science Institute of Madrid, Consejo Superior de Investigaciones Científicas, Madrid 28049, Spain
[∥]King Fahd University of Petroleum and Minerals, Dhahran 34464, Saudi Arabia
[⊥]Faculty of Chemistry, University of Science, VNU-HCM, Ho Chi Minh City 721337, Vietnam

Ⓢ *Supporting Information*

ABSTRACT: A crystalline material with a two-dimensional structure, termed metal–organic framework-901 (MOF-901), was prepared using a strategy that combines the chemistry of MOFs and covalent–organic frameworks (COFs). This strategy involves *in situ* generation of an amine-functionalized titanium oxo cluster, $Ti_6O_6(OCH_3)_6(AB)_6$ (AB = 4-aminobenzoate), which was linked with benzene-1,4-dialdehyde using imine condensation reactions, typical of COFs. The crystal structure of MOF-901 is composed of hexagonal porous layers that are likely stacked in staggered conformation (**hxl** topology). This MOF represents the first example of combining metal cluster chemistry with dynamic organic covalent bond formation to give a new crystalline, extended framework of titanium metal, which is rarely used in MOFs. The incorporation of Ti(IV) units made MOF-901 useful in the photocatalyzed polymerization of methyl methacrylate (MMA). The resulting polyMMA product was obtained with a high-number-average molar mass (26 850 g mol^{-1}) and low polydispersity index (1.6), which in many respects are better than those achieved by the commercially available photocatalyst (P-25 TiO_2). Additionally, the catalyst can be isolated, reused, and recycled with no loss in performance.

In the chemistry of carboxylate metal–organic frameworks (MOFs), the chelation of the carboxyl organic linker to metal ions gives metal-carboxyl clusters, secondary building units (SBUs), which act as anchors ensuring the overall architectural stability of the MOF.[1] Although many of these SBUs are known as discrete clusters, it has been difficult to directly use them as starting building blocks for MOFs.[2] The main reason is the sensitivity of cluster formation to reaction conditions and, in many cases, the incompatibility of such conditions with those required for MOF synthesis and crystallization.[3] This limitation has prevented access to the vast, diverse, and well-developed cluster chemistry[4] and the potential richness of properties they would provide to MOFs.

In this contribution, we articulate a strategy for making discrete metal clusters *in situ* that are appropriately functionalized to affect imine-condensation reactions, commonly used in the chemistry of covalent–organic frameworks (COFs).[5] We find that the chemistry of cluster formation and COFs, when carried out in sequence, overcome the challenge of synthetic incompatibility.

Inspired by the chemistry of hexameric titanium oxo clusters,[6] we reasoned that it is possible to functionalize a known cluster with amine functionalized carboxyl ligands (Scheme 1). Indeed, this allows the resulting cluster to be

Scheme 1. Synthetic Scheme Depicting the Generalized Formation of a Discrete Hexameric Titanium Cluster, Which Can Be Appropriately Functionalized with Amine Groups To Affect Imine Condensation Reactions[a]
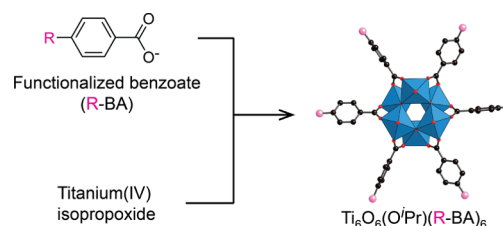
[a]Atom colors: Ti, blue; C, black; O, red; R groups, pink; H atoms and capping isopropoxide units are omitted for clarity.

linked together through imine condensation reactions. Initial synthetic attempts were performed in a sequential, stepwise manner, in which a discrete, isolated Ti(IV) cluster, $[Ti_6O_6(O^iPr)_6(AB)_6]$ (AB = 4-aminobenzoate; O^iPr = isopropoxide), was first synthesized according to previous reports.[6a] Based on reticular chemistry, this hexagonal building block has six points-of-extension and when linked with a linear linker would lead to an **hxl** layered topology.[7] Thus, titanium(IV) isopropoxide $[Ti(O^iPr)_4]$ and 4-aminobenzoic

acid (H-AB) were reacted under solvothermal conditions in isopropanol (see Supporting Information (SI), Section S2). After successful synthesis and full characterization of the cluster, exhaustive efforts were undertaken to form the corresponding MOF upon reactions with benzene-1,4-dialdehyde (BDA). However, due to the low solubility of the cluster in a variety of solvents, only poorly crystalline powders or amorphous solids were obtained. Accordingly, a one-pot synthetic approach, with BDA present, was performed given the fact that the synthetic conditions to form the hexameric $[Ti_6O_6(O^iPr)_6(AB)_6]$ were found to be robust (Figure 1).
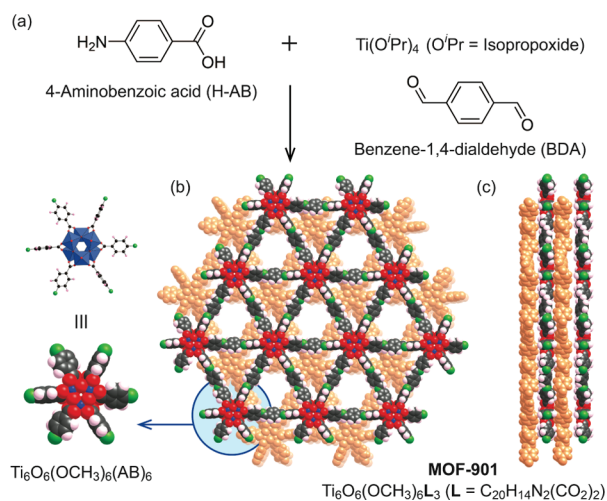

Figure 1. MOF-901 was synthesized by exploiting the robust conditions used to form the discrete hexameric Ti(IV) oxo cluster. In forming MOF-901, 4-aminobenzoic acid was judiciously chosen to generate *in situ* amine-functionalized hexameric clusters, which were, in turn, stitched together through imine-condensation reactions involving benzene-1,4-dialdehyde (a). The crystal structure of MOF-901 is projected along the *c*-axis (b) and *a*-axis (c). The discrete hexameric cluster, now incorporated into an extended, crystalline structure, is presented in the inset of (b). Atom colors: Ti, blue; C, black; O, red; N, green; H, pink; and second layer, orange. Capping methoxide moieties are removed for clarity.

A one-pot mixture containing $Ti(O^iPr)_4$, H-AB, and BDA in methanol was solvothermally reacted in a sealed tube (N_2 atmosphere) at 125 °C for 3 days to yield a yellow microcrystalline MOF-901 (Figure 1). The microcrystalline MOF-901 was subsequently washed with N,N-dimethylacetamide prior to any further analysis in order to remove unreacted starting material. It is noted that the formation of metal oxide (TiO_2) impurities is a real possibility when synthesizing Ti-based MOFs; thus, a density separation was performed using bromoform to ensure that the as-synthesized MOF-901 was pure.[8] The resulting purified material was then activated at 130 °C for 24 h, under dynamic vacuum (1 mTorr), to remove guest molecules residing within the pores (2.9 mg of activated product collected, 33.9% yield based on $Ti(O^iPr)_4$; SI, Section S3).

We initially examined the underlying structural features of MOF-901 using Fourier transform infrared analysis (FT-IR) to prove the imine formation and ^{1}H nuclear magnetic resonance (NMR) spectroscopy to gain a better understanding of the cluster composition (SI, Sections S4 and S5). The formation of the imine functionalities was clearly revealed in the FT-IR spectrum of activated MOF-901. Specifically, the presence of

characteristic imine-derived C=N ($v_{C=N}$ = 1625.9 cm^{-1}) and C−C=N−C ($v_{C-C=N-C}$ = 1199.7 cm^{-1}) stretching vibration frequencies was observed whereas these frequencies were absent in the FT-IR spectra of the isolated hexameric cluster and starting materials. Furthermore, there was a notable absence of the aldehyde-originating stretching band ($v_{C=O}$ = 1685 cm^{-1}) that would result from a partially reacted BDA. ^{1}H NMR spectroscopy on an acid-digested sample revealed a singlet resonance at 3.5 ppm with an integrated value of 3 protons, which was attributed to the presence of methoxide functionalities. Interestingly, there was no resonance observed for isopropoxide leading to the conclusion that methoxide moieties capped the hexameric cluster.

Structural elucidation of MOF-901 was carried out by powder X-ray diffraction analysis (PXRD) using a synchrotron radiation source (SI, Section S6). The experimental diffraction patterns exhibited low-angle diffraction peaks with no evidence of the starting materials or discrete clusters (Figure 2). The
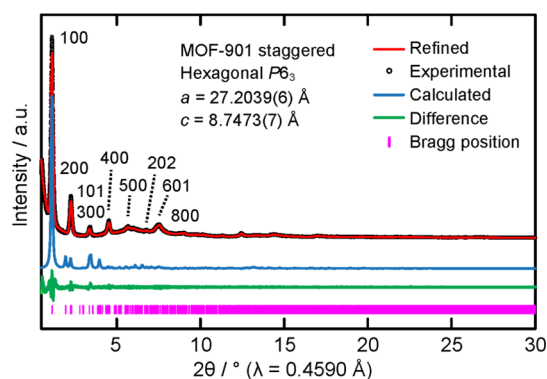

Figure 2. PXRD analysis of activated MOF-901 displaying the experimental pattern (black), refined Pawley fitting (red), and calculated pattern from the staggered structural model (blue). The difference plot (green) and Bragg positions (pink) are also provided.

experimental pattern was then indexed in a primitive hexagonal system ($P6_3$, No. 173) with unit cell parameters, a = 27.4037 and c = 8.9403 Å. Given the connectivity of the SBUs and linkers and to understand the lattice packing of MOF-901, structural models based on the **hxl** topology were generated using *Materials Studio 6.0* software. The proposed 2D structure of MOF-901 was first modeled with two extreme possibilities of stacking modes of the layers: (i) A stacking sequence with both layers fully eclipsed (modeled in the trigonal space group *P*-3, No. 147). A lower symmetry space group was utilized for this model in order to avoid overlapping of the asymmetric units. (ii) A staggered stacking sequence (modeled in the hexagonal space group $P6_3$, No. 173). This model was generated by translating every second layer along the (xy) plane by a/$\sqrt{3}$ Å (where a = 27.2 Å, the distance of two hexameric titanium clusters on the same layer). The translation allowed the hexameric titanium cluster of the second layer to be located in the center of the triangular window generated from the first layer (Figure 1). After a geometrical energy minimization of the structural models, diffraction patterns were simulated and compared with the experimental diffraction patterns obtained for MOF-901; agreement was observed with the staggered conformational model (Figure 2). A full profile Pawley fitting was performed in order to achieve the final unit cell parameters (a = 27.2039(6) and c = 8.7473(7) Å) leading to satisfactory agreement factors and acceptable profile differences. We note

that the disappearance of some experimental peaks (most notably, [2 −1 0] and [2 0 1]) was detected in comparison with the simulated pattern from the staggered model. This is anticipated, as MOF-901 is a layered structure, in which there is a real possibility of an imperfect stacking sequence (inclined or turbostratic disorder). Ultimately, the low data resolution precluded the use of Rietveld refinement to fully assign the stacking sequence. It is noted that this is often the case for the related class of materials, COFs.[5]

The geometry of the proposed SBU in MOF-901 is composed of a trigonal prismatic Ti_6O_6 inner core, in which the octahedral Ti atoms are divided evenly over two separate triangular planes and bound to one another, in corner-sharing fashion, through 6 μ_3-O atoms (Scheme 1). The inner core is surrounded by six equatorial, planar, and chelating terminal AB ligands. This arrangement affords the SBU with six points-of-extension in the shape of a hexagon. Finally, capping the top and bottom of the inner core are six methoxide moieties. When linked together through imine condensation reactions with BDA, the resulting extended structure contains triangular windows, 14 Å in width, and an interlayer spacing of ca. 3.47 Å (Figure 1). With respect to the topology, MOF-901 has one vertex, represented by the $Ti_6O_6(-CO_2)_6$ SBU, and one edge (linker) leading to a 3^6 faced **hxl** topology.

To further support and formulate the character of MOF-901, scanning electron microscopy (SEM), elemental microanalysis (EA), thermogravimetric analysis (TGA), and N_2 adsorption measurements were performed on an activated sample of MOF-901 (SI, Sections S7−S9). Accordingly, SEM analysis demonstrated a small particle size whose crystal morphology was ambiguous due to aggregation of smaller crystallites, but nevertheless appeared homogeneous in nature (SI, Section S9). In terms of chemical formulation of MOF-901, EA data revealed the chemical formula of MOF-901 to be $Ti_6O_6(OCH_3)_6L_3$ (where L = $C_{20}H_{14}N_2(CO_2)_2$), Calcd: C, 51.46; H, 3.60; N, 5.00% and found: C, 51.10; H, 3.28; N, 5.23%, which is in line with the formula derived from the proposed structure. TGA supported the derived chemical formula as determined by EA as well as the high thermal stability of the material (200 °C). Specifically, the TiO_2 residue (32.3 wt %) was found to be close to the theoretical TiO_2 value (28.6 wt %) that was calculated from the modeled crystal structure. Furthermore, the weight loss percentage (67.7 wt %) originated at 450 °C was attributed to, and consistent with, the imine-formed organic linker and the capping methoxide moieties (71.4 wt % based on the modeled structure). Finally, the permanent porosity of MOF-901 was examined by N_2 adsorption measurements at 77 K. The resulting Brunauer−Emmett−Teller surface area of MOF-901 was calculated to be 550 m^2 g^{-1}. It is noted that this value is in agreement with the theoretical specific surface area calculated for the staggered model of MOF-901 (650 m^2 g^{-1}; SI, Section S8).

Given the high likelihood of the new material's photoresponsiveness, based on the integration of Ti atoms within the framework, we sought to analyze the photoactivity of MOF-901 (SI, Section S10). Accordingly, UV−vis diffuse reflectance spectroscopy was performed, in which the absorption range extended from 340 to 550 nm with the absorption maximum located at 360 nm. As expected, from the yellow color of MOF-901, this material absorbs light in the visible region. The calculated band gap, based on the Tauc plot, was found to be 2.65 eV. This band gap is slightly larger than that calculated for PCN-22 (1.93 eV)[3a] and similar to Ti-MIL-125-NH$_2$ (2.6 eV).[9]

The charge transfer process, and thus the demonstration of successful generation and separation of electron−hole pairs, was analyzed by photoluminescence spectroscopy. Under laser irradiation at 365 nm, MOF-901 exhibited a broad luminescent band centered at 484 nm. Mott−Schottky measurements were then performed to understand the conductivity and flat band potential of MOF-901. The results indicated a negative slope revealing the fact that MOF-901 can be described as a p-type semiconductor with a flat band potential of 0.57 V vs Ag/AgNO$_3$.

Encouraged by these findings, we sought to demonstrate the photocatalytic activity of MOF-901. We used MOF-901 as a photocatalyst in the visible light mediated radical polymerization of methyl methacrylate (MMA) with a co-initiator, ethyl α-bromophenylacetate (SI, Section S11). Initially, we focused on optimizing the catalyst loading, co-initiator quantity, and reaction time. As shown in Table 1, a catalyst and co-initiator

Table 1. Photocatalyzed Polymerization of Methyl Methacrylate (MMA) under Visible Light Irradiation
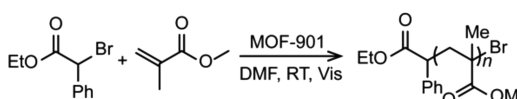
entry	catalyst [mol %]	yield [%]	M_n [g mol^{-1}]	M_w/M_n
MOF-901[a]	0.034	87	26 850	1.6
P-25 TiO$_2$[a]	0.034	52	17 000	1.6
[Ti$_6$O$_6$(O^{i}Pr)$_6$(AB)$_6$][a]	0.034	n.d.	n.a.	n.a.
MOF-901[b]	0.034	n.d.	n.a.	n.a.
Blank[c]	0	n.d.	n.a.	n.a.
MIL-125-NH$_2$[a]	0.034	n.d.	n.a.	n.a.
VNU-1[a]	0.034	n.d.	n.a.	n.a.
UiO-66-NH$_2$[a]	0.034	13	18 500	1.6

[a]Reaction conditions: MMA (2.0 M in N,N-dimethylformamide), catalyst (0.034 mol %), and ethyl α-bromophenylacetate (0.61 mol %) at rt with visible light from a compact fluorescent lamp (4U, 55 W) for 18 h. [b]Reaction performed in the absence of light irradiation. [c]Reaction performed without catalyst. n.d. = not detected; n.a. = not applicable; M_n = number-average molar mass; M_w = mass average molar mass.

loading of 0.034 and 0.61 mol % (with respect to MMA), respectively, and a reaction time of 18 h was found to be ideal. The optimized conditions resulted in polymerization with a high molecular weight of polyMMA (26 850 g mol^{-1}), high yield (87%), and reasonable distribution, as indicated by a low polydispersity index (PDI) of 1.6. Control experiments were subsequently performed in order to assess the photocatalytic activity of MOF-901. As expected, there was no observable product when the discrete [Ti$_6$O$_6$(O^{i}Pr)$_6$(AB)$_6$] cluster was used, nor in the absence of catalyst (i.e., blank sample) or visible light.

MOF-901 clearly outperforms Degussa P-25 TiO$_2$ in producing high molecular weight (M_n) polyMMA product (Table 1). Here, MOF-901 affords a polyMMA product whose M_n (26 850 g mol^{-1}) was 1.5 times higher than that of the commercially available Degussa P-25 TiO$_2$ (17 000 g mol^{-1}). Additionally, the gel permeation chromatogram (GPC) of the polyMMA product is more uniform when MOF-901 is used, owing to a higher degree of control over the polymerization process. It is also noted that the activity of MOF-901 is higher than previously reported photocatalysts employed in this

reaction, especially with respect to the larger molecular weight of the resulting polyMMA and lower PDI value achieved.[10] To further demonstrate MOF-901's high performance, comparative experiments were performed using the photocatalysts MIL-125-NH$_2$,[9] VNU-1,[11] and UiO-66-NH$_2$,[12] who all possess similar band gap energies as MOF-901. Interestingly, there was no polyMMA product detected when VNU-1 and MIL-125-NH$_2$ were employed as the photocatalyst (Table 1). On the contrary, UiO-66-NH$_2$ was demonstrated to promote the polymerization of MMA, albeit the polyMMA product was achieved in significantly lower yield (13%) and molecular weight (M_n = 18 500 and 26 850 g mol^{-1} for UiO-66-NH$_2$ and MOF-901, respectively) than MOF-901 (Table 1).

The heterogeneous nature of MOF-901 was validated through recycling experiments. Upon conclusion of the reaction, MOF-901 was isolated by centrifugation and washed several times with dichloromethane before regeneration under vacuum (1 mTorr) (SI, Section S11). PXRD analysis of this regenerated material revealed that the structure of MOF-901 was maintained. The photoinitiated polymerization reaction was then performed again under identical conditions. The activity of MOF-901 remained, without any loss of performance, over at least three consecutive cycles. Indeed, this recyclability further demonstrates the outperformance of MOF-901 versus other MOFs used for polymerization purposes.

■ ASSOCIATED CONTENT

Ⓢ Supporting Information

The Supporting Information is available free of charge on the ACS Publications website at DOI: 10.1021/jacs.6b01233.

> Synthesis and characterization of MOF-901, PXRD analysis data, including computational modeling, and photocatalysis measurements details and data (PDF)

■ AUTHOR INFORMATION

Corresponding Author

*yaghi@berkeley.edu

Notes

The authors declare no competing financial interest.

■ ACKNOWLEDGMENTS

■ REFERENCES

(1) (a) Luebke, R.; Belmabkhout, Y.; Weselinski, L. J.; Cairns, A. J.; Alkordi, M.; Norton, G.; Wojtas, L.; Adil, K.; Eddaoudi, M. Chem. Sci. 2015, 6, 4095. (b) Alezi, D.; Peedikakkal, A. M. P.; Weseliński, Ł. J.; Guillerm, V.; Belmabkhout, Y.; Cairns, A. J.; Chen, Z.; Wojtas, Ł.;

Eddaoudi, M. J. Am. Chem. Soc. 2015, 137, 5421. (c) Furukawa, H.; Cordova, K. E.; O'Keeffe, M.; Yaghi, O. M. Science 2013, 341, 1230444.
(2) (a) Wang, K.; Feng, D.; Liu, T.-F.; Su, J.; Yuan, S.; Chen, Y.-P.; Bosch, M.; Zou, X.; Zhou, H.-C. J. Am. Chem. Soc. 2014, 136, 13983. (b) Feng, D.; Wang, K.; Wei, Z.; Chen, Y.-P.; Simon, C. M.; Arvapally, R. K.; Martin, R. L.; Bosch, M.; Liu, T.-F.; Fordham, S.; Yuan, D.; Omary, M. A.; Haranczyk, M.; Smit, B.; Zhou, H.-C. Nat. Commun. 2014, 5, 5723. (c) Liu, Y.; Eubank, J. F.; Cairns, A. J.; Eckert, J.; Kravtsov, V. C.; Luebke, R.; Eddaoudi, M. Angew. Chem., Int. Ed. 2007, 46, 3278.
(3) (a) Yuan, S.; Liu, T.-F.; Feng, D.; Tian, J.; Wang, K.; Qin, J.; Zhang, Q.; Chen, Y.-P.; Bosch, M.; Zou, L.; Teat, S. J.; Dalgarno, S. J.; Zhou, H.-C. Chem. Sci. 2015, 6, 3926. (b) Bueken, B.; Vermoortele, F.; Vanpoucke, D. E. P.; Reinsch, H.; Tsou, C.-C.; Valvekens, P.; De Baerdemaeker, T.; Ameloot, R.; Kirschhock, C. E. A.; Van Speybroeck, V.; Mayer, J. M.; De Vos, D. Angew. Chem., Int. Ed. 2015, 54, 13912.
(4) Guillerm, V.; Gross, S.; Serre, C.; Devic, T.; Bauer, M.; Férey, G. Chem. Commun. 2010, 46, 767.
(5) (a) Uribe-Romo, F. J.; Hunt, J. R.; Klock, C.; O'Keeffe, M.; Yaghi, O. M. J. Am. Chem. Soc. 2009, 131, 4570. (b) Zhang, J.; Liu, L.; Liu, H.; Lin, M.; Li, S.; Ouyang, G.; Chen, L.; Su, C.-Y. J. Mater. Chem. A 2015, 3, 10990. (c) Huang, N.; Krishna, R.; Jiang, D. J. Am. Chem. Soc. 2015, 137, 7079. (d) Zhu, Y.; Wan, S.; Jin, Y.; Zhang, W. J. Am. Chem. Soc. 2015, 137, 13772. (e) Zhou, T.-Y.; Xu, S.-Q.; Wen, Q.; Pang, Z.-F.; Zhao, X. J. Am. Chem. Soc. 2014, 136, 15885. (f) Fang, Q.; Gu, S.; Zheng, J.; Zhuang, Z.; Qiu, S.; Yan, Y. Angew. Chem., Int. Ed. 2014, 53, 2878. (g) Duhović, S.; Dincă, M. Chem. Mater. 2015, 27, 5487.
(6) (a) Hong, K.; Chun, H. Inorg. Chem. 2013, 52, 9705. (b) Hong, K.; Bak, W.; Chun, H. Inorg. Chem. 2014, 53, 7288. (c) Rozes, L.; Sanchez, C. Chem. Soc. Rev. 2011, 40, 1006. (d) Papiernik, R.; Hubert-Pfalzgraf, L. G.; Vaissermann, J.; Henriques Baptista Goncalves, M. C. J. Chem. Soc., Dalton Trans. 1998, 2285.
(7) (a) O'Keeffe, M.; Peskov, M. A.; Ramsden, S. J.; Yaghi, O. M. Acc. Chem. Res. 2008, 41, 1782. (b) Yaghi, O. M.; O'Keeffe, M.; Ockwig, N. W.; Chae, H. K.; Eddaoudi, M.; Kim, J. Nature 2003, 423, 705.
(8) (a) Bae, Y.-S.; Dubbeldam, D.; Nelson, A.; Walton, K. S.; Hupp, J. T.; Snurr, R. Q. Chem. Mater. 2009, 21, 4768. (b) Sudik, A. C.; Millward, A. R.; Ockwig, N. W.; Côté, A. P.; Kim, J.; Yaghi, O. M. J. Am. Chem. Soc. 2005, 127, 7110.
(9) (a) Nasalevich, M. A.; Goesten, M. G.; Savenije, T. J.; Kapteijn, F.; Gascon, J. Chem. Commun. 2013, 49, 10575. (b) de Miguel, M.; Ragon, F.; Devic, T.; Serre, C.; Horcajada, P.; García, H. ChemPhysChem 2012, 13, 3651. (c) Hendon, C. H.; Tiana, D.; Fontecave, M.; Sanchez, C.; D'arras, L.; Sassoye, C.; Rozes, L.; Mellot-Draznieks, C.; Walsh, A. J. Am. Chem. Soc. 2013, 135, 10942.
(10) Although MOF-901 outperforms the photocatalysts reported in the following references, especially with regard to the polyMMA product's yield, larger molecular weight, and lower PDI value, the varying conditions reported for these photocatalytic polymerizations make direct comparisons challenging. (a) Wang, Z. J.; Landfester, K.; Zhang, K. A. I. Polym. Chem. 2014, 5, 3559. (b) Uemura, T.; Ono, Y.; Kitagawa, K.; Kitagawa, S. Macromolecules 2008, 41, 87. (c) Kiskan, B.; Zhang, J.; Wang, X.; Antonietti, M.; Yagci, Y. ACS Macro Lett. 2012, 1, 546. (d) Fors, B. P.; Hawker, C. J. Angew. Chem., Int. Ed. 2012, 51, 8850.
(11) Doan, T. L. H.; Nguyen, H. L.; Pham, H. Q.; Pham-Tran, N.-N.; Le, T. N.; Cordova, K. E. Chem. - Asian J. 2015, 10, 2660.
(12) Long, J.; Wang, S.; Ding, Z.; Wang, S.; Zhou, Y.; Huang, L.; Wang, X. Chem. Commun. 2012, 48, 11656.
(13) (a) Uemura, T.; Kitagawa, K.; Horike, S.; Kawamura, T.; Kitagawa, S.; Mizuno, M.; Endo, K. Chem. Commun. 2005, 5968. (b) Vitorino, M. J.; Devic, T.; Tromp, M.; Férey, G.; Visseaux, M. Macromol. Chem. Phys. 2009, 210, 1923. (c) Inokuma, Y.; Nishiguchi, S.; Ikemoto, K.; Fujita, M. Chem. Commun. 2011, 47, 12113. (d) Uemura, T.; Mochizuki, S.; Kitagawa, S. ACS Macro Lett. 2015, 4, 788.